

RESEARCH LETTER

Open Access



Modeling the impacts of projected climate change on wheat crop suitability in semi-arid regions using the AHP-based weighted climatic suitability index and CMIP6

Karam Alsafadi¹ , Shuoben Bi^{1*} , Hazem Ghassan Abdo^{2,3} , Hussein Almohamad⁴, Basma Alatrach⁵, Amit Kumar Srivastava⁶ , Motrih Al-Mutiry⁷, Santanu Kumar Bal⁸ , M. A. Sarath Chandran⁸  and Safwan Mohammed^{9,10} 

Abstract

Due to rapid population growth and the limitation of land resources, the sustainability of agricultural ecosystems has attracted more attention all over the world. Human activities will alter the components of the atmosphere and lead to climate change, which consequently affects crop production badly. In this context, wheat is considered an important crop and ranks as one of the top strategic crops globally. The main objective of this research is to develop a new approach (a weighted climatic suitability index) for evaluating the climate suitability for wheat production. The specific objectives are to project the impact of future climate change on wheat suitability using three models based on WCSI and CMIP6-based projections and to identify the most vulnerable area to climate change and productivity reduction. The climatic criteria for wheat production were selected and classified into eight indicators based on the Sys' scheme and the FAO framework, and then the weighted overlay approach was used in conjunction with the analytic hierarchy process. To confirm the reliability of the integrated WCSI, we determined the nonlinear curve fitting of integrated WCSI-induced wheat yields by the exponential growth equation. Finally, the CMIP6-GCMs projected from three shared socioeconomic pathways were used for WCSI mapping and predicting wheat yields in the short and long term (Southern Syria was selected as a case study). The results show that the nonlinear correlation between wheat yields and the integrated WCSI was 0.78 ($R^2 = 0.61$) confirming the integrated WCSI's reliability in reflecting yield variation caused by climate suitability. The results indicated that WCSI for wheat will be lower over the study area during 2080–2100 compared to the current climate. During 2080–2100, the wheat yield is projected to decrease by 0.2–0.8 t. ha⁻¹ in the western parts of the study area. The findings of this study could be used to plan and develop adaptation strategies for sustainable wheat production in the face of projected climate change. The results of the study will also help in the strategic planning of wheat production in Syria under the projected climate. The results of this research are limited to small areas as a case study, although they are not relevant to similar regions worldwide. However, the study employs novel analytical methods that can be used broadly.

Keywords Climate change, CMIP6, Yield forecasting, Agro-climatic indices, Agricultural sustainability

*Correspondence:

Shuoben Bi
bishuoben@163.com

Full list of author information is available at the end of the article



© The Author(s) 2023. **Open Access** This article is licensed under a Creative Commons Attribution 4.0 International License, which permits use, sharing, adaptation, distribution and reproduction in any medium or format, as long as you give appropriate credit to the original author(s) and the source, provide a link to the Creative Commons licence, and indicate if changes were made. The images or other third party material in this article are included in the article's Creative Commons licence, unless indicated otherwise in a credit line to the material. If material is not included in the article's Creative Commons licence and your intended use is not permitted by statutory regulation or exceeds the permitted use, you will need to obtain permission directly from the copyright holder. To view a copy of this licence, visit <http://creativecommons.org/licenses/by/4.0/>.

Introduction

In this era, the sustainability of the agricultural ecosystem has attracted more attention all over the world, due to rapid population growth and the limitation of land resources (Abd-Elmabod et al. 2020). In this sense, an acceleration of the global increase in food demand and climate change place great pressure on ecosystem services and global food security (Fanzo et al. 2018). Furthermore, the rainfall patterns are expected to be changed in many regions as a direct consequence of climate change; while some areas will face extreme precipitation events, others will receive less amount of rainfall and an increase in the frequency, intensity, and duration of drought (Kharin et al. 2018; Alsafadi et al. 2020b; Mohammed et al. 2020c; Mokhtar et al. 2021a). Therefore, the agricultural systems in many regions will be significantly affected by land degradation (erosion and desertification) and will have a serious impact on human activities and food security, leading to migration (Mullan 2013; Wheeler & Von Braun 2013; Molotoks et al. 2021; Hateffard et al. 2021). To cope with that dilemma, the United Nations (UN) through its sustainable development goals (SDGs) (i.e., SDG 2 (zero hunger), SDG 13 (climate action), SDG 15 (life on land)) has emphasized the necessity for sustainable use of terrestrial ecosystems under ongoing climate change (Arana et al. 2020; United Nations 2015; Le Blanc 2015).

Many sectors are affected by climate change, for instance, the energy sector (Dowling et al. 2013), the agricultural sector (Hanif et al. 2010), transportation (Koetse, & Rietveld 2009), insurance sector (Botzen et al. 2010), tourism (Seetanah, & Fauzel 2018), agricultural market (Costinot et al. 2016), food supply (Rosenzweig & Parry 1994), and economy (Tol 2013). The agricultural sector was classified as one of the most vulnerable sectors to climate change (Peltonen-Sainio et al. 2010; Parker et al. 2019), where the frequency of extreme climate events (such as droughts) has significantly increased (Alsafadi et al. 2020b; Mokhtar et al. 2021a) and badly affected the crop production, especially in semi-arid and arid regions (Bal and Minhas 2017; Mokhtar et al. 2021b; Harsányi et al. 2021; Alvar-Beltrán et al. 2022). In this context, semi-arid and arid regions covering one-third of the world's land are being used mostly for crop production (Barton et al. 2014) and support 14.4% of the world's population (Huang et al. 2016). Ecosystems in these regions are delicate and vulnerable to intense interactions between human activity and climate change (Huang et al. 2010), where most lands are used for agricultural purposes (Huang et al. 2016). However, a warmer climate accompanied by drought will accelerate evapotranspiration and will

have a tremendous impact on this region, including the Mediterranean Basin (Peltonen-Sainio et al. 2010).

Recently, the Mediterranean Basin's environmental concerns have been compounded by accelerated climate change (Seker and Gumus 2022), where the average temperature is 1.4 °C higher compared to the values in the late 1800s (Cramer et al. 2018), along with successive drought events and heat waves (Mathbout et al. 2021; Alsafadi et al. 2022b). Hence, the eastern part of the Mediterranean Basin was more vulnerable to climate change (Mesta et al. 2022). In this context, a rapid increase in air temperature and decreasing trend of precipitation will negatively affect crop production (Bal et al. 2022a; Al-Bakri et al. 2011). In Syria, the agricultural system is suffering from serious land degradation (Mohammed et al. 2022a), such as soil erosion (Mohammed et al. 2020a, 2020b; Alsafadi et al. 2022c), associated with miss management of land resources and climate change (Mohammed et al. 2020d). However, climate change, especially drought, badly affected the agricultural sector in Syria and led to reduced crop yield all over the country. In this context, wheat is considered an important crop to support self-reliance, which ranks as one of the top strategic crops, with over 1.7 million hectares.

In this context, predicting wheat yields is a key factor for policymakers and agricultural managers so that they can modify their strategies to an expected level of crop production and set suitable plans of adaptation (Ben-Ar et al. 2016; Chen et al. 2018; Reidsma et al. 2009).

A wide variety of methods have been developed for estimating the agro-climatic indices needed to feed models for wheat yield simulation and suitability during the crop growth cycle and assessing the impact of climate change. For instance, the analog and empirical models for durum wheat yield forecasting (Ferrise et al. 2015), the water stress index (WSI) as a daily water balance model (Chourghal et al. 2016), the drought and overwhelmed water key indicator (DOWKI) (Kapsambelis et al. 2019), STICS soil-crop model by coupling gridded datasets of soil and climate (Brisson et al. 2002; Yang et al. 2020), the integrated climatic suitability, which reflects the influence of solar radiation, temperature, and precipitation on the winter wheat suitability in the entire crop growth cycle (Tang and Liu 2021), and several other agro-climatic indices, such as agricultural reference index for drought (ARID) (Woli et al. 2012). More recently, several studies have applied machine learning and deep learning models to predict wheat yield based on meteorological, crop phenological, and remote sensing data (Murakami et al. 2021; Srivastava et al. 2022; Wang et al. 2020; Lischeid et al. 2022). Yet, these methods are rarely assessed for their degree of reliability and have been compared

independently (Ben-Ar et al. 2016; Basso and Liu 2019; Lischeid et al. 2022). Importantly, the overmentioned agro-climatic indices encompass a considerable range of intricacy levels, and several are applied to set the yield forecasts. No single index performs systematically completely (whatever the farming type), hence no obvious relationship between the level of intricacy of indices and their reliability (Ben-Ar et al. 2016).

The models previously referred to can be classified into three key types: crop simulation models or biophysical models; statistical data-based regression models; and functional models (Kirthiga and Patel 2022; Basso and Liu 2019). Not all the models can evaluate the spatial-temporal climatic suitability for a specific crop and forecast the yield accurately at the same time, and they cannot all transact with the climate change projection data from general circulation models because it depends on the inputs and their availability. The biophysical model is a process-based simulation model that accounts for the interaction between environmental information and its effect on the crop rather than using statistical or functional models, such as sowing date, grain size, soil properties, and other management practices in addition to weather information (Kirthiga and Patel 2022; Asseng et al. 2014). Such a process-based approach results in highly accurate simulation of crop yields but in countries, such as Syria, where long historical records on the crop parameter values and crop management practices are not available, as a result, the biophysical models become inapplicable, in short, it is suffering from complexity, needing intensive parameters, and therefore difficult to calibrate and parameterize (Basso and Liu, 2019). However, the regression models are less parameter intensive and simple. These models fit the direct relationship between meteorological parameters and crop yield and can be considered to have good efficiency and satisfying output (Mathieu and Aires 2018; Srivastava et al. 2022), but they cannot assess specifically the climatic crop suitability of a single meteorological parameter at each phenological stage (e.g., the meteorological drought indices). The functional-based models, which define the agro-meteorological requirements based on crop suitability theory and the analytic process methods and fuzzy logic, can be used to analyze the suitability of a single meteorological parameter at each phenological stage and play an important role in examining the climatic suitability for a specific crop (Tang and Liu 2021). But these models cannot deal with the possible discrepancy in agro-meteorological criteria priorities, mainly when selecting a weight for each indicator.

Our study suggests an approach that combines the advantages of functional-based models in defining the weighted agro-meteorological requirements to evaluate

the spatial-temporal climatic suitability and regression-based models to forecast the crop yield accurately. This approach also seeks to sidestep some of the more unsettling limitations in the complex biophysical models and transacts with the climate change projection data from general circulation models to estimate the impact of climate change. Thus, the goal of this research was to create an approach for evaluating the climate suitability for wheat cultivation and yield forecasting and apply it as a case study in southern Syria. The specific objectives are 1) to evaluate the suitability of the current climate for wheat cultivation in southern Syria; 2) to project the impact of future climate change on wheat suitability using three models based on a weighted climatic suitability index and Coupled Model Intercomparison Project Phase 6 (CMIP6) General circulation model (GCM)-based projections; and 3) to identify the most vulnerable and sensitive area to climate change in terms of wheat suitability in the eastern Mediterranean.

Materials and methodology

Study area

Our research was carried out in southwestern Syria near the Jordanian border, between latitudes 32° 18' and 33° 15' North and longitudes 35° 45' and 37° 25' East (an area of 10236.2 Km²) (Fig. 1) which represents the upper and middle portion of the Yarmouk basin. The study area is characterized by a continental climate. Spatially, the average summer temperature is between 18 and 32 °C in July, while the winter average is between 3 and 10 °C in January. The regional mean annual precipitation is 283 mm,

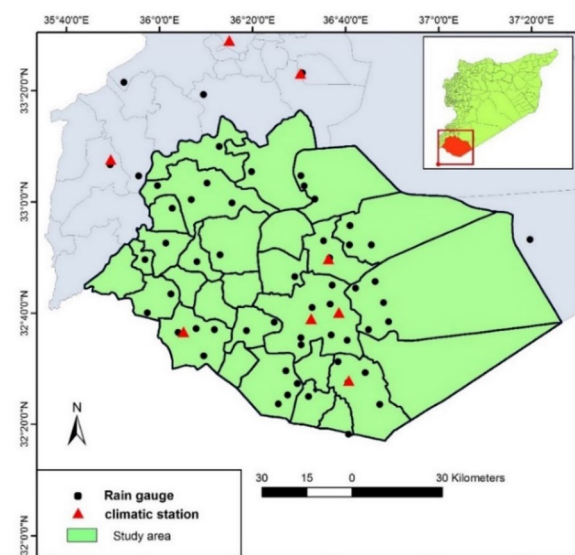


Fig. 1 The study area and location of the rain gauge and climatic stations

with maximum precipitation of about 550 mm in the mountains area (for the spanning period of 1982–2015). According to the Köppen-Geiger classification, the study area is located in the temperate wet climate C (i.e., Csa and Csb) in the western and central heights areas. In contrast, the climate is arid (Desert) and semi-arid (Steppe) B (i.e., Bw and Bs) in the lower areas and toward the east (Beck et al. 2018). The region is divided into three physiographical units: mountains in the central area (Jabal Al Arab) and plateaus in the northwestern part (Golan heights extent), while a plain area in most of the study area (Horan plain), where the altitude ranges between 1809 m above sea level in the central part and - 5 m below sea level in the western part. The major agricultural land use in the area incorporates apples (*Malus sylvestris*), grapes (*Vitis sp*), olive (*Olea europaea*), tomatoes (*Lycopersicon Esculentum*), and wheat (*Triticum spp*).

According to the Ministry of Agriculture and Agrarian Reform (MoAAR) in Syria, the cultivated area of wheat reached about 110 thousand hectares with a production of about 134.6 thousand tons in 1995. While it reached about 76.6 thousand hectares with a production of about 48 thousand tons in 2015. This area is considered one of the most significant regions in Syria in producing “durum wheat,” which is well-known and renowned for its high gluten component (Al-Saleh and Brennan 2012).

Climatic data and pre-processing

Current climate and projected climate change of the Coupled Model Intercomparison Project Phase 6) CMIP6) for monthly temperature and precipitation spanning 1961–2000 and 2020–2100, respectively, were acquired from the WorldClim dataset at 1 km² (30 arc-s) spatial resolution for baseline data and 5 km² (2.5 arc-min) for downscaled climate change (Hijmans et al. 2005; Fick et al. 2017). Downscaled monthly gridded data of average temperature and precipitation were used for three global climate models (GCMs) in Table 1: BCC-CSM2-MR, CanESM5, and IPSL-CM6A-LR under three Shared Socio-economic Pathways (SSPs), 126, 245, and 585, for two periods, 2020–2040 and 2080–2100 (<https://www.worldclim.org>).

Given that the baseline gridded data of WorldClim precipitation have biased values and uncertainties, which are

increasingly associated with the interpolation techniques compared to local observations (Alsafadi et al. 2021), the bias correction method was implemented to this end as presented in Fig. 2a–c. The bias correction is generally applied for generating a relationship between the observed variables and modeled ones using spatial interpolation of the residuals. It was done based on in situ data from 57 rain gauges from the Syrian Meteorological Authority (SMA), the MoAAR, taking into consideration the stations located inside and outside the study area as shown in Fig. 1. All of these data were collected and computed at a monthly time scale for the span of 1982–2015.

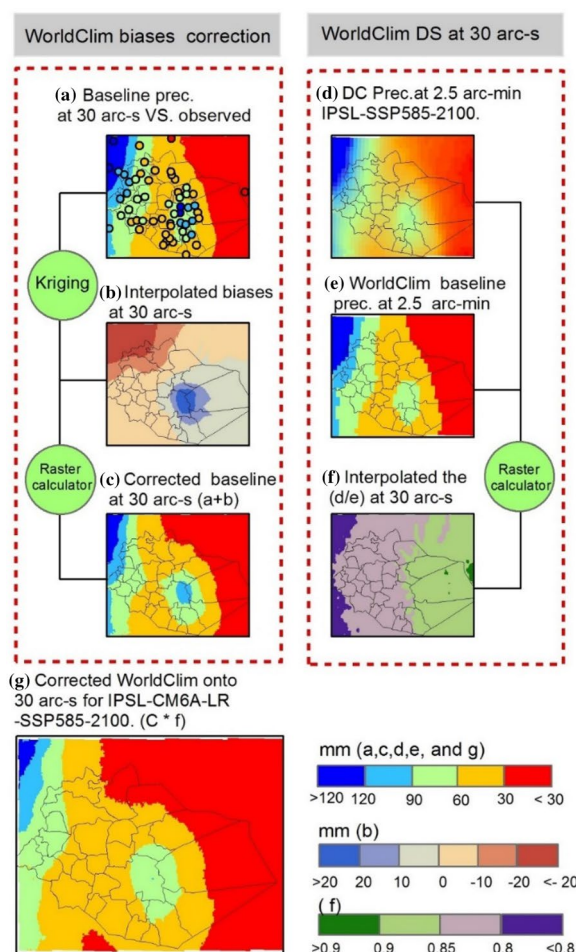


Fig. 2 Illustration of the WorldClim biases correction process for January precipitation (values in mm/month) using local dataset. (a) WorldClim-baseline data at 30 arc-s and observed data, (b) interpolated biases at 30 arc-s and observed data, (c) corrected-baseline data, (d) WorldClim future data for the2090s (2080–2100 average) under SSP858 at 2.5 arc-min, (e) WorldClim-baseline data at 2.5 arc-min, (f) interpolated relative future data to the baseline data or relative anomaly surface by 2100 at 30 arc-s, (g) future corrected and downscaled climate surface at 30 arc-second spatial resolution

Table 1 CMIP6 models used in this study

No	Model	Center	Resolution
1	BCC-CSM2-MR	Beijing climate center (China)	1.125° × 1.125
2	CanESM5	Canadian centre for climate modeling and analysis (Canada)	2.81° × 2.81
3	IPSL-CM6A-LR	Institute pierre simon laplace (France)	2.5° × 1.26

This gridded precipitation data were used for further calculation in this research.

To acquire bias-corrected and high spatial resolution surfaces of CMIP6 projections for climate change at 30 arc-s, the downscaling (DC) method (Navarro-Racines et al. 2020; Xu et al. 2021) was used as a simple approach to biases correction in which a “delta method” or change factor is derived from the GCMs, and then added onto the baseline climate (observation-corrected WorldClim data). The DC method includes the following steps (Fig. 2d–f): (1) calculation of temperature and precipitation averages for baseline climate and near and far future periods (2020–2040 and 2080–2100); (2) computation of anomalies as the absolute difference between future and baseline values in average temperatures and relative differences in amounts of precipitation (Fig. 2f); (3) interpolation of these anomalies at 30 arc-s using Kriging method for GCMs gridded points; and (4) addition of the interpolated anomalies data to the baseline from WorldClim.

Weighted climatic suitability index

Definition of agro-climatological requirements

In this study, climatic criteria of wheat production were selected and classified into eight indicators that fall within a unified level, as illustrated by Mohammed et al. (2020d) based on the Sys’ scheme (Sys et al. 1993) and the FAO framework (FAO 1976) (Fig. 3). Our study labeled each wheat climatic requirement into five categories: an extremely suitable class (S1), an acceptable suitable class (S2), a moderately suitable class (S3), a tentatively unsuitable class (N1), and a completely unsuitable class (N2) (FAO 1976).

In the next step, we assigned the degree of limitation (Rank of criterion *xi*) for each layer on a 0–4 rating scale, then merged it with the AHP weights. As such, the Weighted Overlay Approach (WOA) (Voogd et al. 1982) was used to create weighted climatic suitability as

$$S = \left[\sum_{i=1}^n wi * xi \right], \tag{1}$$

$$WCSI = 100 + \left(-2.55 * S^3 \right) + \left(6.071 * S^2 \right) + \left(-9.28 * S \right),$$

wi: Weight of criterion *ixi*: Rank of criterion *i*, for each layer on a 0–4 rating scale. *WCSI*: Weighted Climatic suitability index in percentage, which is defined by the nonlinear relationship between the rating scale (%) and degree of limitation (Fig. 3).

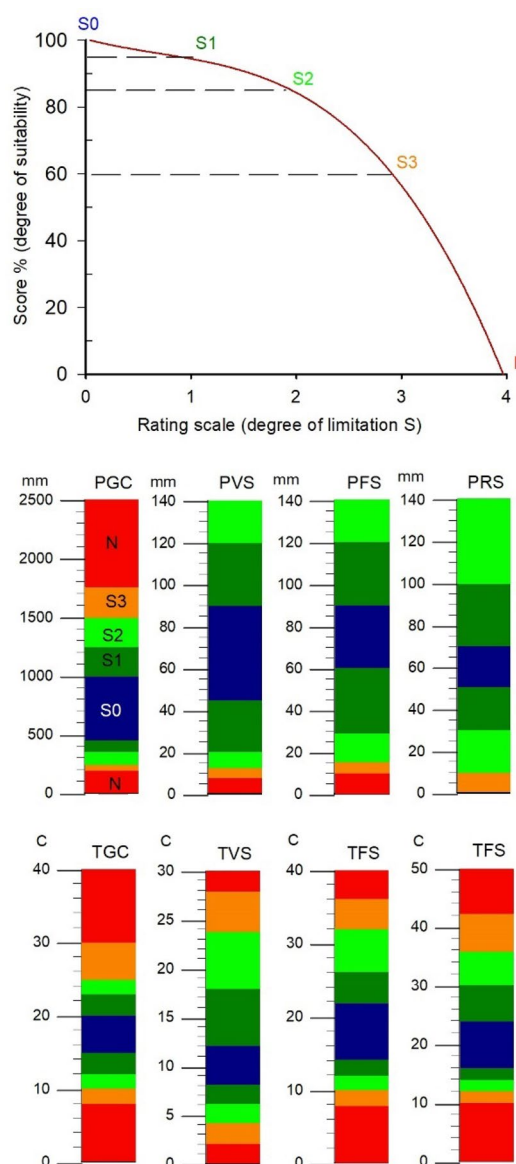


Fig. 3 The upper scheme is the nonlinear curve fitting between the score of suitability (WCSI) and the 0–4 rating scale, or the degree of limitation. Climatic requirements for wheat cultivation, based on the Sys’ table (Sys et al. 1993). Note: PGC, precipitation of growing cycle (Oct to May); PVS, precipitation of vegetative stage (Mar); PFS, precipitation of flowering stage (Apr); PRS, precipitation of ripening stage (May); TGC, mean temp. of the growing cycle (Nov to May); TVS, mean temp. of the vegetative stage (Mar); TFS, mean temp. of the flowering stage (Apr); TRS, Mean temp. of the ripening stage (May)

Determination of climatic indicators weightage

Even though the Geographic Information Systems (GIS)-based linear layers combination technique has been considered an essential tool in processing geospatial data, the application of this tool alone could not transact with the possible discrepancy in criterion priority, mainly when

selecting a weight for each indicator (Alsafadi et al. 2022a). To this end, the Analytic Hierarchy Process (AHP) method is utilized in conjunction with the linear overlay method or combination technique within the GIS environment (Feizizadeh and Blaschke 2013; Mugiyo et al. 2021). The AHP is an acknowledged decision support system for environmental management (Alsafadi et al. 2020a) that was introduced by Saaty (1977), which provides a statistical scale of decision consistency, arranges preference levels among criteria hierarchically, and simplifies priority levels among criteria using pair-wise comparisons, particularly when processing complicated decisional matters (Saaty 1980, 1990, 2008).

Herein, the preference ratios of climatic indicators were assigned initially from a pair-wise partial correlations (PCorr) matrix of the selected criteria (climatic indicators) against observed yields for a span of 2000–2015 to set the relative importance of a specific indicator compared to other indicators, then rounded to the nearest whole number, i.e., converting it to the Saaty’s 1 to 9 scale ratios (Saaty and Vargas 1991) to assign a pair-wise comparison matrix (PWCM) as

$$R_x = \begin{cases} \frac{PCorr_{xi}}{PCorr_{xn}} \text{ (if } PCorr_{xi} > PCorr_{xn}); \text{ More importance} \\ 1 \text{ (if } PCorr_{xi} = PCorr_{xn}); \text{ equal importance} \\ \frac{1}{\left(\frac{PCorr_{xi}}{PCorr_{xn}}\right)} \text{ (if } PCorr_{xi} < PCorr_{xn}); \text{ Less importance} \end{cases}, \tag{2}$$

where R_x is the score value and the PCorr matrix has the property of reciprocity as an essential judgment expressed by $1/x_i$.

Through a PWCM, the AHP calculates the weight of each indicator (W_i) by getting the Eigenvector identical to the largest Eigenvalue of the matrix and then normalizing the aggregate of the elements to unity as

$$\sum_{i=1}^n W_i = 1. \tag{3}$$

The primary input is elements of the PWCM, matrix A , which can be acquired as a matrix of n indicators created based on Saaty’s 1 to 9 scale ratios which are of the regulation $n \times n$ and expressed as

$$A = [a_{ij}], i, j = 1, 2, 3, \dots, n, \tag{4}$$

in which A is a PWCM with components a_{ij} . The matrix A has the property of reciprocity as an essential rule, which can be illustrated by $a_{ij} = 1/a_{ji}$. Subsequently, the total values in each column of the matrix A were

computed to normalize the primary PWCM, which can be expressed mathematically by $(\sum_{i=1}^n a_{ij} = 1, 2, 3, \dots, n)$.

After completing the components of the primary matrix (A), we normalized it as a matrix B , which can be defined as

$$B = [b_{ij}], i, j = 1, 2, 3, \dots, n, \tag{5}$$

in which matrix B is the normalized primary matrix (A), and its elements (b_{ij}) can be obtained as

$$b_{ij} = a_{ij} / \sum_{i=1}^n a_{ij} = 1, 2, 3, \dots, n \tag{6}$$

Each weight (W_i) was calculated by dividing the total values of the b_{ij} within the matrix rows by the total number of factors or indicators (n):

$$W_i = \frac{\sum_{j=1}^n b_{ij}}{\sum_{j=1}^n \sum_{i=1}^n b_{ij}}, i, j = 1, 2, 3, \dots, n. \tag{7}$$

Equations (E1), (E2), (E3), (E4), and (E5) in the appendices demonstrate the relationships between the principal Eigenvalue (λ_{max}) and the corresponding

Eigenvector (W) of the normalized matrix (Chen et al. 2010; Feizizadeh et al. 2014; Saha et al. 2021).

Ultimately, to demarcate the final wheat climatic suitability map, the eight thematic layers of the climatic indicators were integrated using Eq. (1) and the raster calculator in ArcGIS tools (see Fig. 4). In a later step, the nonlinear curve fitting of integrated WCSI-induced yields is calculated by exponential growth equation as follows:

$$y = a * \exp^{(b * WCSI)}$$

Wheat yields dataset in the statistical yearly report issued by the AMAS (2000–2021) and the climatic dataset collected from the SMA were used to analyze the relationship between the wheat yield ($t \cdot h^{-1} \cdot yr^{-1}$) and the integrated WCSI. The yield data from 2000 to 2015 period was used for calibration against the WCSI and 2016–2021 data for testing against the future WCSI from ensemble CMIP6 GCMs.

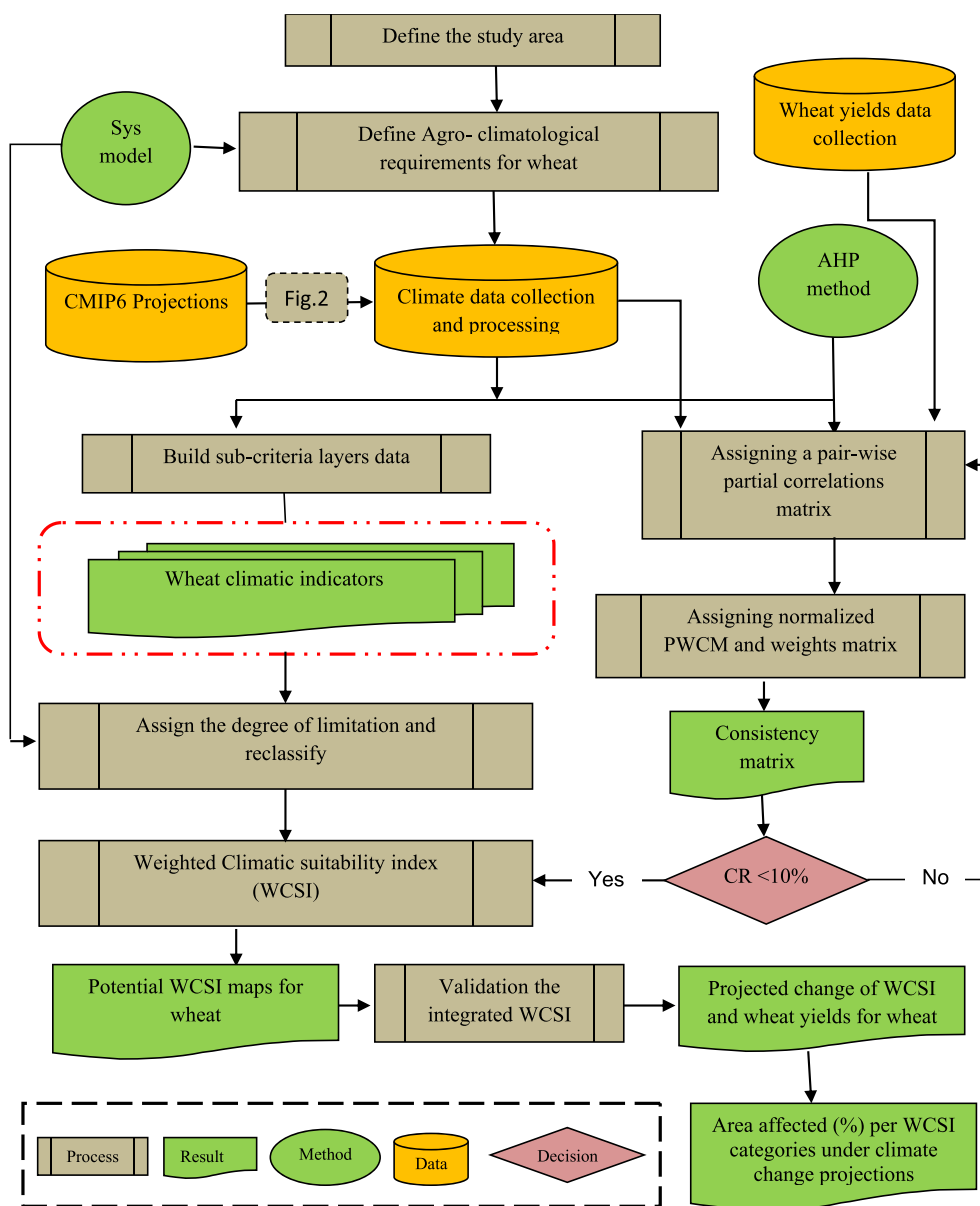


Fig. 4 Flowchart of the methodology applied for the analysis of the WCSI for wheat cultivation under climate change projections

Results

Normalized PWCM and weights of agro-climatological variables

The normalized PWCM and normalized weight amounts of the climatic variables were used in this study according to Saaty’s approach in weights selection, as shown in Tables 2 and 3. As provided, the CR value of the paired comparison is less than 10%, which is utilized in conjunction with the values of the maximum Eigenvalue, CI, and RI to indicate that the decision’s consistency is acceptable for the pairwise comparisons. The weight values for the climatic

parameters of rainfed wheat production show that the PGC is the most important criterion, with a weight value of 0.26–0.4 and a positive relationship with wheat growth and yields, followed by the PVS and TFS. The weight values of the PFS and TGC, on the other hand, are the least important criterion, with a value of < 0.08.

Assessment of the WCSI against wheat yields and CMIP6 GCMs’ predictability

The WCSI is assumed to be positively linked to wheat growth and yields. Herein, we calibrated and tested

Table 2 Normalized PWCM for climatic parameters of rainfed wheat for the eastern part of the study area (Swaida)

Criteria	TGC	TVS	TFS	TRS	PGC	PVS	PFS	PRS	W _j	Consistency	
TGC	0.07	0.07	0.07	0.14	0.06	0.07	0.08	0.07	0.08	8.45	
TVS	0.07	0.07	0.07	0.14	0.06	0.07	0.08	0.07	0.08	8.45	
TFS	0.07	0.07	0.07	0.14	0.06	0.07	0.08	0.07	0.08	8.41	
TRS	0.01	0.01	0.01	0.02	0.05	0.02	0.01	0.01	0.02	8.09	
PGC	0.46	0.46	0.46	0.14	0.42	0.40	0.41	0.43	0.40	8.63	
PVS	0.20	0.20	0.20	0.14	0.21	0.20	0.17	0.21	0.19	8.56	
PFS	0.07	0.07	0.07	0.14	0.08	0.10	0.08	0.07	0.08	8.38	
PRS	0.07	0.07	0.07	0.14	0.07	0.07	0.08	0.07	0.08	8.44	
λ _{max} =8.43; n=8; CI=0.06; RCI=1.41; CR=0.044 < 0.1. The constancy of the judgement is satisfactory										Σ=1	Avg=8.43

Table 3 Normalized PWCM for climatic parameters of rainfed wheat for the western part of the study area (Daraa)

Criteria	TGC	TVS	TFS	TRS	PGC	PVS	PFS	PRS	W _j	Consistency	
TGC	0.03	0.04	0.03	0.03	0.02	0.03	0.05	0.03	0.03	8.71	
TVS	0.10	0.11	0.38	0.10	0.05	0.11	0.12	0.11	0.13	8.79	
TFS	0.22	0.06	0.19	0.20	0.42	0.21	0.21	0.21	0.22	8.79	
TRS	0.10	0.11	0.10	0.10	0.05	0.21	0.05	0.21	0.12	8.62	
PGC	0.29	0.44	0.10	0.41	0.21	0.21	0.21	0.21	0.26	8.84	
PVS	0.13	0.11	0.10	0.05	0.11	0.11	0.14	0.11	0.11	8.67	
PFS	0.02	0.02	0.02	0.05	0.02	0.02	0.02	0.01	0.02	8.87	
PRS	0.13	0.11	0.10	0.05	0.11	0.11	0.19	0.11	0.11	8.63	
λ _{max} =8.74; n=8; CI=0.1; RCI=1.41; CR=0.075 < 0.1. The constancy of the judgement is satisfactory										Σ=1	Avg=8.74

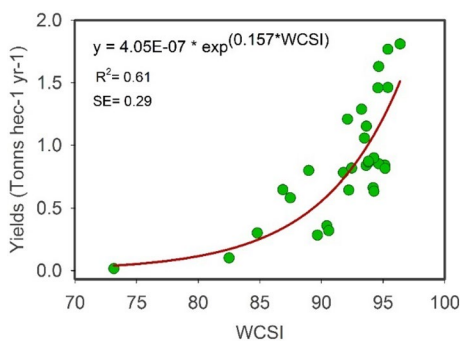


Fig. 5 Fitting the nonlinear relationship between the yields ($t \cdot h^{-1} yr^{-1}$) and the integrated WCSI for 2000–2015

the WCSI and wheat yields in the whole study area. The WCSI-induced yield can reflect the variation that will be caused by climate change and was utilized to confirm the reliability of the integrated WCSI. For the 2000–2015 period, the results show the nonlinear correlation coefficient (r) between the wheat yields and the integrated WCSI at Swaida and Daraa was 0.78, whereas R^2 was 0.61 at $p < 0.01$ significant level with a standard error of 0.29 $t \cdot h^{-1}$ (Fig. 5). We tested the predictability of the wheat yield and the WCSI using the ensemble GCMs' data during the testing period of 2016–2021. The results indicate that the correlation (r) and R^2 between observed and predicted wheat yields using ensemble GCMs under scenario SSP585 were 0.52 and 0.22, respectively, whereas the correlation (r) and R^2 between observed and predicted WCSI for the same scenario were 0.58 and 0.32, respectively (Table 4). This indicates that the SSP585 scenario had a higher probability to capture the variability of climate and wheat yields in the study area. The SSP245 scenario, on the other hand, showed a reverse relationship for WCSI prediction and less predictability of the crop yield (See Fig. 6).

Projected change of precipitation and temperature during the wheat growing cycle

The spatial distribution of precipitation during the wheat growing cycle (PGC) for 1982–2015 and projected

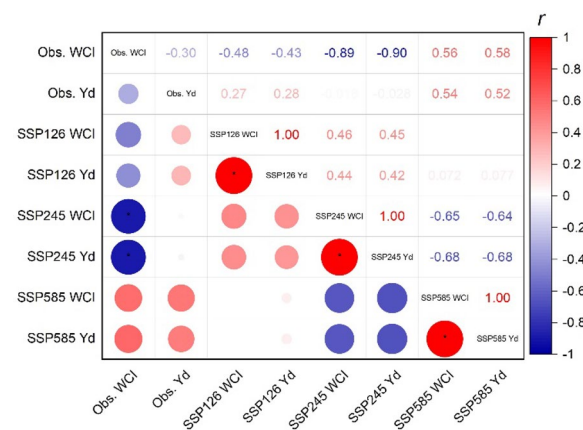


Fig. 6 The correlation matrix between observed WCI and wheat yields and predicted ones by GCMs' SSP scenarios for the testing period of 2016–2021

change for 2020–2100 under the scenarios SSP126, SSP245, and SSP585 are shown in Fig. 7.

The spatial distributions of PGC for 1982–2015 are similar to BCC-CSM2-MR projections under SSP245 scenario with a slight decrease, but the PGC presented more decline compared with 1982–2015 for Canadian and French models under the SSP585 scenario. As such, the boundary of the PGC for 2080–2100 shifts westward, and the suitability in the central and western parts of the study area is less compared with the baseline. Projected change of PGC by most GCMs utilized in the study area suggested somewhat a consistent declining pattern in the regional mean PGC values, but these declines are more pronounced under the SSP585 scenario, i.e., the aggressive emissions scenario.

The spatial distribution of temperature during cycle (TGC) for 1982–2015 and projected change for 2020–2100 under SSP126, SSP245, and SSP585 are presented in Fig. 8.

The spatial distributions of TGC for 1982–2015 are near to GCMs projections under SSP126 for the 2020–2040 period with a slight increase, but the TGC presented more increases compared with 1982–2015 for CanESM5 and IPSL-CM6A-LR under the SSP585 scenario, as such,

Table 4 Summary of testing the ensemble GCMs' predictability of the yield and the WCSI data during the 2016–2021 period

		Predicted by GCMs SSP126	Predicted by GCMs SSP245	Predicted by GCMs SSP585
Observed WCSI	r	0.48	- 0.89	0.58
	R^2	0.23	0.79	0.32
Observed yield	r	0.30	- 0.03	0.52
	R^2	0.1	0.01	0.22

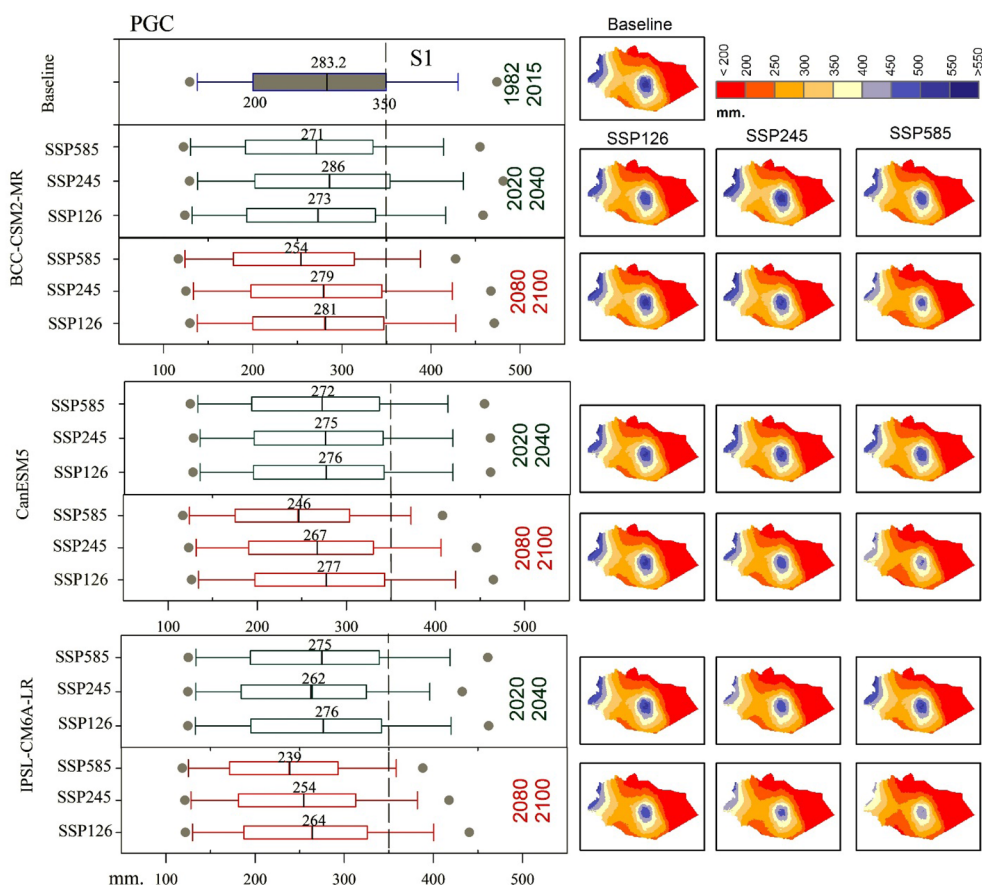


Fig. 7 Spatial distribution projected change of precipitation during the wheat growing cycle (PGC) derived from three CMIP6 GCMs

the boundary of the TGC for 2080–2100 shifting from S1 class to S0 class, where the suitability in the study area is higher compared with the baseline. Projected change of TGC by most GCMs utilized in the study area indicated the same patterns of increases in the regional mean of TGC values, but these increases are more pronounced for CanESM5 and IPSL-CM6A-LR under the SSP585, i.e., the aggressive emission scenario of 2080–2100 period; hence, the boundary of the TGC returns to S1 class but linked with an aggressive increase in temperature values.

Temporal evolution of the WCSI and wheat yield under current climate and CMIP6 GCMs ensemble

Figure 9 shows the temporal evolution of the WCSI and wheat yield from 1982 to 2015, as well as the projected change for 2022–2100 under scenarios SSP126, SSP245, and SSP585. The temporal evolution of the WCSI for 1982–2015 presented a slight decrease, and the biggest decrease was in 2008. While the temporal evolution of the WCI and wheat yield under ensemble CMIP6 GCMs and SSPs presented varied projections, for instance, the WCSI recorded lower values than the baseline in the

SSP585 scenario. This indicates that the WSCI and wheat yields will be more affected by warming and decreasing precipitation under SSP245 and SSP585 scenarios, i.e., the aggressive emissions scenarios.

Spatial distribution of the WCSI

The spatial distribution of rainfed wheat’s WCSI for the baseline 1982–2015 and time periods 2020–2040 and 2080–2100 under the scenarios SSP126, SSP245, and SSP585 is presented in Fig. 10 and Table 5. The WCSI for the baseline 1982–2015 ranges from 75 to 100% and reveals an increasing trend from east to west. The area with WCSI between 95 and 85% (S2), mainly distributed in most of the study area except the western and central parts, accounting for roughly 77.2% of the study area. However, the area with WCSI higher than 95% (S1) accounts for 13% of the study area.

For GCM “BCC-CSM2-MR,” between 2020 and 2100 under three SSP scenarios, WCSI values decrease in some parts and increase in other parts with WCSI values higher than the baseline and are mostly distributed in the central and western parts, while, the WCSI

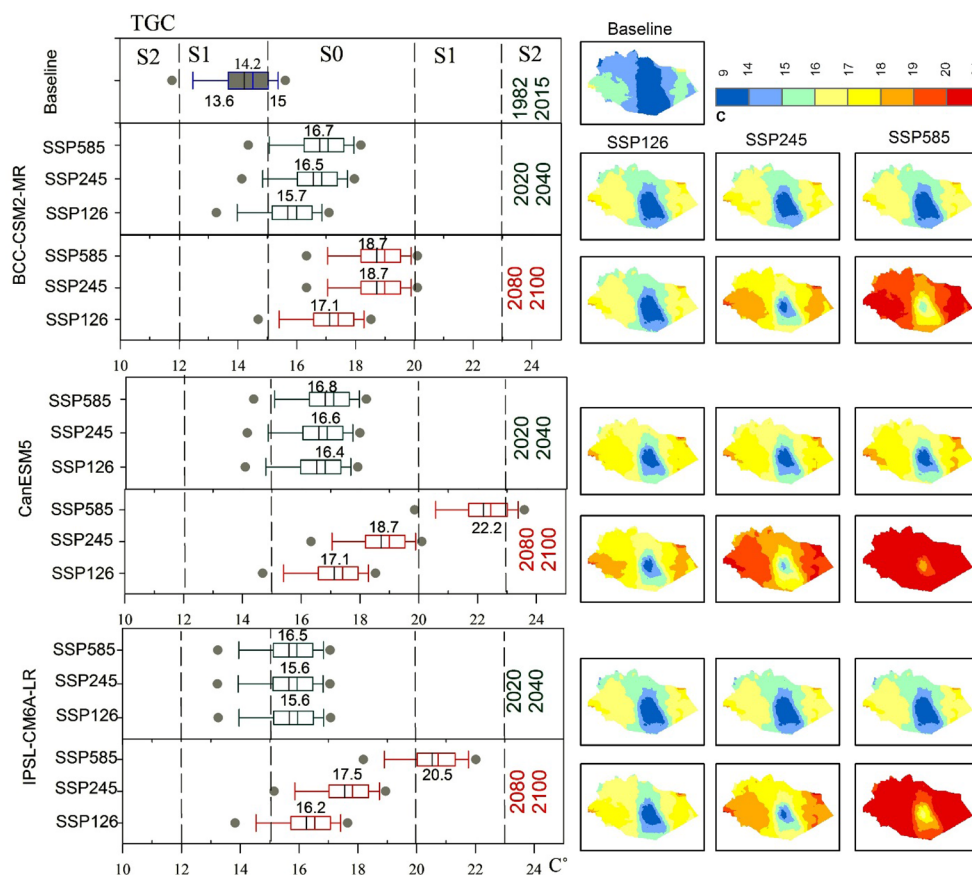


Fig. 8 Spatial distribution projected change of temperature during the wheat growing cycle (TGC) derived from three CMIP6 GCMs

record lower values than baseline in the eastern parts. The area with WSCI values between 85 and 95% (S2) are mainly distributed with an estimated area of 74.7, 73.1, and 66.6% of the study area under the three scenarios SSP126, SSP245, and SSP585, respectively, for 2021–2040, whereas in 2080–2100 the proportions are approximately 80.1, 64, and 63.1% under the three scenarios SSP126, SSP245, and SSP585, respectively. Remarkably, the boundary of the S3 class moves westward and increases in the 2080–2100, covering an area of 19.6 and 30.8% of the study area under SSP245 and SSP585, respectively. Under the SSP585 scenario and 2080–2100 period, the boundary of WCSI for S1 class shrinks greatly in the central and western parts and covers only an area of 6%.

Regarding GCM “CanESM5” projections between 2020 and 2100 under three SSP scenarios, the WSCI values increase and decline in some parts. The area with WSCI values between 85 and 95% (S2) is 64.4, 64, and 64.2% of the study area under scenarios SSP126, SSP245, and SSP585, respectively, for 2021–2040, whereas the

proportions are approximately 60.8, 59.2, and 64.5% under the same three scenarios, respectively, for 2080–2100. Remarkably, the boundary of the S3 class moves westward and increases more broadly than BCC-CSM2-MR in the 2080–2100 period, where this region covers an area of 27.3 and 34.2% of the study area under the scenarios SSP245 and SSP585, respectively. Under the SSP585 scenario and 2080–2100 period, the boundary of WCSI for S1 class shrinks greatly in the central and western parts and covers only an area of 1.3%. Under the SSP245 scenario and the 2080–2100 period, the boundary of WCSI for S2 class shrinks greatly in the central part and covers an area of 59.2%.

According to GCM “IPSL-CM6A-LR” projections for the same periods and scenarios, the WSCI records sharp increasing and decreasing trends in the study area. The area with WSCI values between 95 and 85% (S2) is 66.4, 68.2, and 68.5% of the study area under three scenarios SSP126, SSP245, and SSP585, respectively, for 2020–2040, but the proportion is approximately 67.3, 60.8, and 62.6% under the same three scenarios, respectively, for

2080–2100 period. Remarkably, the boundary of the S3 class clearly moves westward and increases more broadly than BCC-CSM2-MR and CanESM5 in the 2080–2100 period, where this region covers an area of 30.4 and 35.2% of the study area under scenarios SSP245 and SSP585, respectively, while under the SSP585 scenario and 2080–2100 period, the boundary of WCSI for S1 class shrinks largely in the central and western part and covers only an area of 2.2% of the region but it is higher than that in CanESM5 projections.

Compared with the baseline (1985–2015), the class with a WCSI between 60 and 85% (a moderately suitable class) is mainly distributed in the northern and eastern parts, and it will be increased by 21, 24.2, and 25% for 2080–2100 under SSP585 for the three models, respectively, coupled with a decreasing in the S2 class by 14.1, 12.7, and 14.6%, for 2080–2100 under the SSP585 for the three models. According to the CanESM5 and IPSL-CM6A-LR projections, the spatial distributions of WCSI anomalies (Fig. 11) compared to the baseline under RCP8.5 for 2080–2100 indicate that the suitability will decrease in the future by 6–10% in the eastern and northern portions, by 2–6% in the western part, which is conducive to degradation the cultivation of winter wheat. While the BCC-CSM2-MR projection leads to optimistic

reductions with values ranging between 0 and 6% for the same period and scenario.

Spatial distribution of projected wheat yields

The spatial distribution of wheat yields for the baseline 1982–2015 and both periods of 2020–2040 and 2080–2100 under SSP126, SSP245, and SSP585 are presented in (Fig. 12). The yields for the baseline 1982–2015 range from 0.25 to 2 t. ha⁻¹ and reveal an increasing tendency from the east to the west. The area with the lowest values (<0.5 t. ha⁻¹) is mainly distributed in most of the study areas except the western and central parts, whereas the area with a value higher than 1 t. ha⁻¹ is distributed in the western and central parts.

Regarding the three models for 2020–2100 under three scenarios, the wheat yield values decrease in some parts and increase in other parts, with a value higher than the baseline in the central portion, while the area record lower values than the baseline in the eastern portion. Remarkably, the boundary of 0 to 0.5 t. ha⁻¹ class moves westward in the 2080–2100 period under SSP245 and SSP585 scenarios. For IPSL-CM6A-LR projections under the SSP585 scenario in 2080–2100, the boundary of 1.5 to 2 t. ha⁻¹ class shrinks greatly in the central and

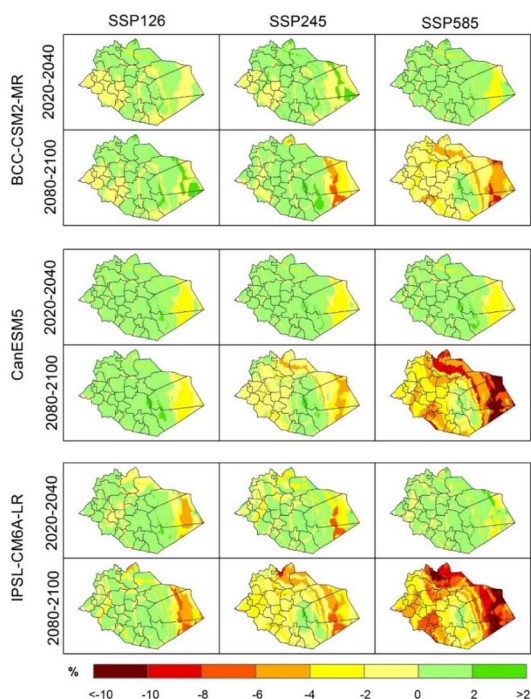


Fig. 11 Spatial distribution of wheat's WCSI anomalies compared to the baseline 1982–2015, for both periods of 2020–2040 and 2080–2100 under SSP 126, SSP 245, and SSP585

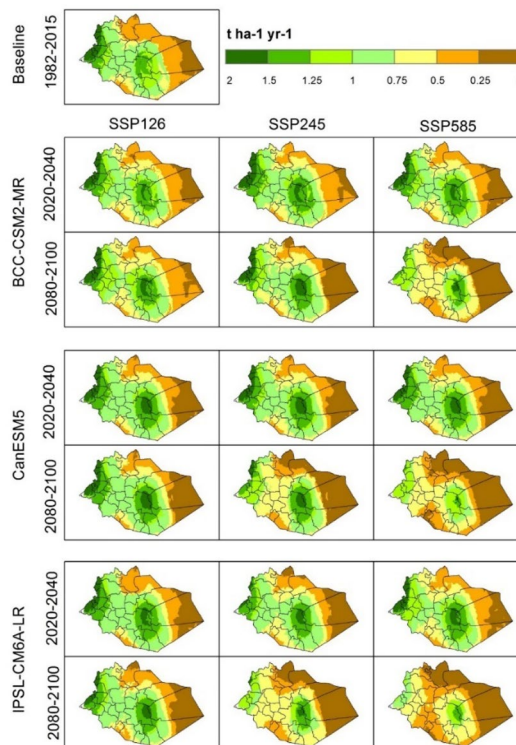


Fig. 12 Spatial distribution of rainfed wheat's productivity for the baseline 1982–2015, and projections climate change for both periods of 2020–2040 and 2080–2100 under SSP126, SSP245, and SSP585

western parts and covers a small area, while the class between 0 and 0.75 t ha⁻¹ moved toward the central parts remarkably.

Compared with the baseline (1985–2015), the yields will be increased by 0.2–0.8 t ha⁻¹ in the central part for 2020–2040 under all scenarios and the three models. According to the CanESM5 and IPSL-CM6A-LR projections, the spatial distributions of yield anomalies under RCP8.5 for the 2080–2100 period (Fig. 13) compared to the baseline indicate that the productivity will decrease in the future by – 0.1 to – 0.2 t ha⁻¹ in the eastern and northern parts, and by – 0.2 to – 0.8 t ha⁻¹ in the western part. However, the results indicate that BCC-CSM2-MR projection would lead to less yield losses for the same period and scenario.

Discussion

The WCSI' predictability of wheat yields, benefits, and limitation

Several studies have presented the importance of climatic data to detect crop productivity and classified the agro-climatic indices into three classes to study this association: crop simulation models or biophysical models (Kotlowski 2007; Kirthiga and Patel 2022); empirical data-based regression models (Lobell et al. 2007); and functional models (Chipanshi et al. 2015).

In our study, we focus on the WCSI as one of the empirical regression models for the prediction of wheat yield. It is less process oriented than crop simulation models and requires fewer auxiliary data compared to biophysical models, such as sowing date, grain size, soil properties, and other management practices (Asseng et al. 2014; Kirthiga and Patel 2022). It is calibrated on historical agro-climatic data during the crop growing season with as little a priori information as possible, which makes it flexible and applicable using climate change projections, which cannot be easily applied using functional and process-based models (Mathieu and Aires 2018; Wallach et al. 2021). It ranked the optimal values of temperature and precipitation during the crop growing season and transferred them to a numerical scale that took into account the optimal values and the critical limits for the growth and productivity of wheat. Simply put, it can be considered a climate indicator based on the optimal and critical values for wheat growth, unlike the meteorological indices that depend on the standardized values of a climatic element and its deviation from the mean. Therefore, the negative values of the meteorological drought index may not reflect the critical limits affecting the yield (Nxumalo et al. 2022), especially in wet climates where the water balance is permanently positive in the higher latitudes. This leads to a negative correlation with the crop yield, which some studies interpret as a main factor for wheat yield losses in these areas due to wet stress (Mokhtar et al. 2021b; Mohammed et al. 2022b). Therefore, considering this type of indicator when estimating may lead to a deterioration in the performance of the outputs; herein, the WCSI works to avoid this limitation by using the functional relationships (optimum curves). This is consistent with what was found by Lischeid et al. (2022); the models yielded an optimum temperature curve for months of the growing season, which indicated harmful impacts of extreme temperatures on yield, particularly during the critical phenological stages, such as grain filling and flowering. On the other hand, Li et al. (2019) found clear harmful effects of extreme precipitation on maize yield, where optimum precipitation in summer and late spring exceeded that of earlier months. However, this contradicts what was discovered by Pirttioja et al. (2015) using the 26 biophysical-based models, which assumed a monotonic increase in wheat yield with increased precipitation in some countries (e.g., Spain, Germany, and Finland), but some studies confirm that most biophysical-based models tend to underestimate the negative impacts of excess precipitation above the optimum limits (Lobell and Asseng 2017; Webber et al. 2020). The optimum curves effects have acquired considerable attention recently in the context of global

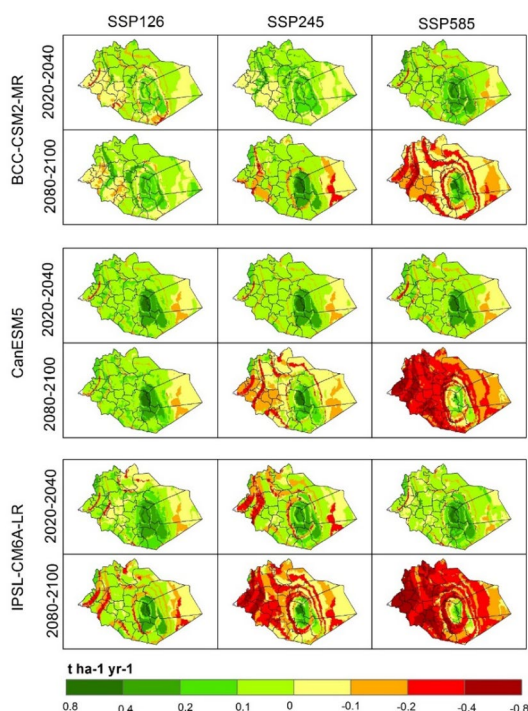


Fig. 13 Spatial distribution of wheat productivity anomalies compared to the baseline 1982–2015, for both periods of 2020–2040 and 2080–2100 under SSP 126, SSP 245, and SSP585

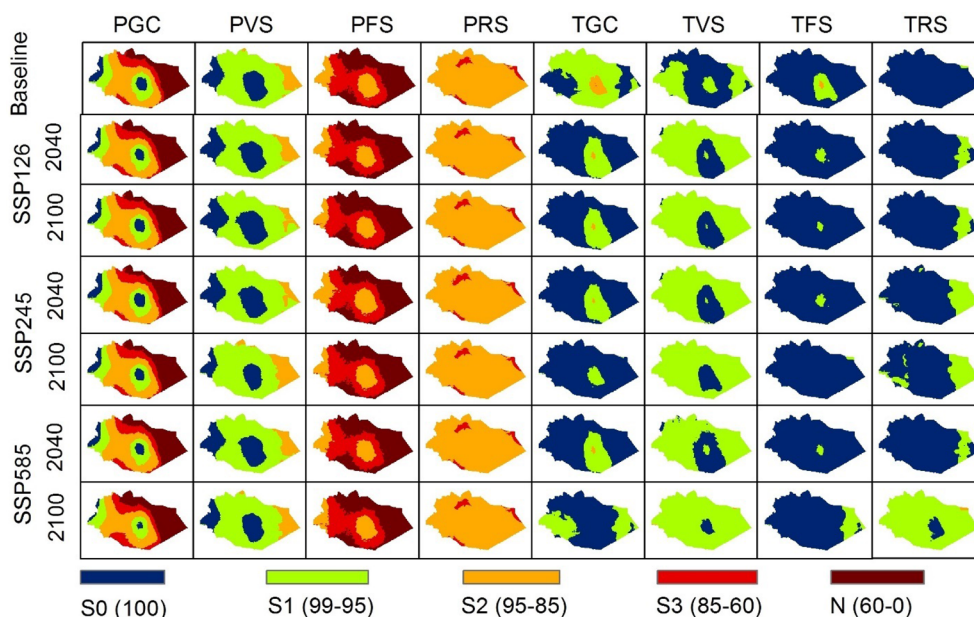


Fig. 14 Projected change of wheat agro-climatological zones during the growing cycle derived from BCC-CSM2-MR

warming and climate change effects, specifically for wheat (Webber et al. 2018).

Although the WCSI presented good outputs in the prediction of wheat yield, it has some limitations: the effects of extreme weather events during the growing season were not taken into consideration in the WCSI's parameters. In this study, the same set of parameters for winter wheat was used for all regions by considering the symmetric distribution of climate. The other major factor affecting yield prediction is the distribution of wheat varieties, whose agro-climatic characteristics (optimal values) could show some variations across the regions, and leading to uncertainties in their climate suitability, thus uncertainties in yield prediction. As such, adding new parameters, such as phenological data and sowing periods, and their application on a local scale needs further study in the future. However, presenting an integrated approach to crop yield modeling is a pivotal point for a better understanding of the potential impacts of climate change on crops, such as wheat, to develop appropriate mitigation strategies under climate change conditions.

Climate change and its effect on wheat production

Climate change has adversely affected the agricultural sector all over the world on both the global and regional scales (Ahmad et al. 2015, 2019; Abbas et al. 2017; Liu et al. 2018). The southern part of Syria is subjected to climate change, especially drought, which had a negative impact on the agricultural sector and led to

a decrease in crop yield, particularly in the first decade of the twentieth century (Mohammed et al. 2020c). In this research, the impact of current and future climate (2020–2040, 2080–2100) on wheat production was assessed by using a new approach "the Weighted Climatic Suitability Index" under future climate data derived from three different GCMs (BCC-CSM2-MR, CanESM5, and IPSL-CM6A-LR). The results revealed that the baseline climate is moderately suitable (S2) for wheat production (Table 5). Previously, Mohammed et al. (2020d) reported that both precipitation and temperature were suitable (S1) for wheat production in the southern part of Syria. The differences between current research and Mohammed et al. (2020d) could be mainly explained by the implementation of the new approach (i.e., WCSI) based on AHP weights and WLC.

Regardless of the model that was implemented, climate change will pose a major threat to wheat production in the southern part of Syria (Table 5, and Fig. 13). Nonetheless, the BCC-CSM2-MR was more optimistic than the other models in terms of climate suitability for wheat production in southern Syria, as can be detected in the Appendices (Figs. 14, 15, and 16). However, the differences in the model's prediction can be explained by the difference in the inputs that are used in each model to simulate the feedback of the ecosystem on climate and climate change. In this context, the CanESM5 was reported to be one of the pioneer models with coarse resolution and high equilibrium climate sensitivity (Swart et al. 2019). Global climate models are expecting

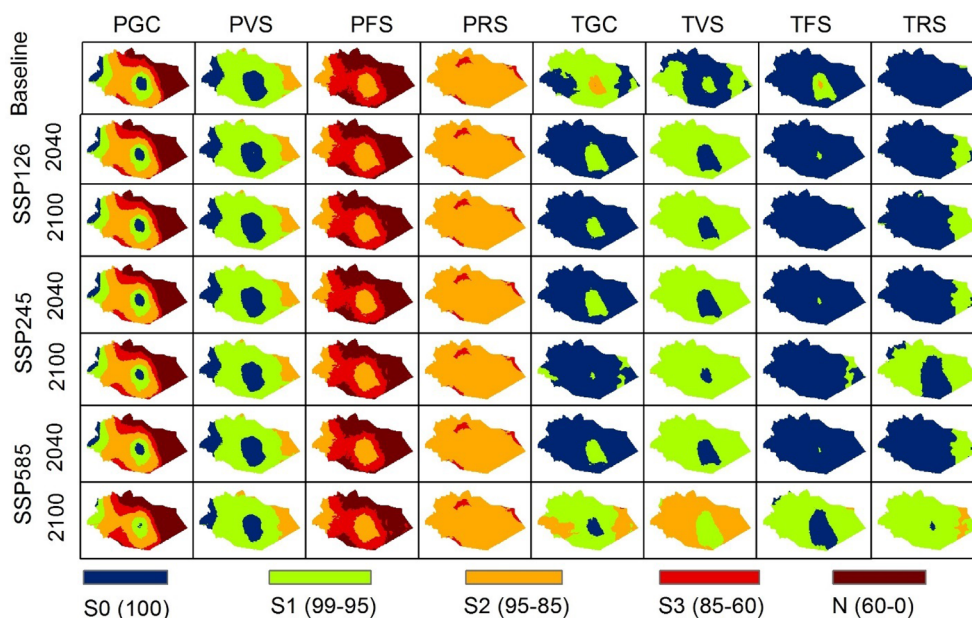


Fig. 15 Projected change of wheat agro-climatological zones during the growing cycle derived from CanESM5

an increase in the earth’s temperature along with an increased level of CO₂ concentration, which will have a different impact on crop production (Emam et al. 2015). On one hand, elevated CO₂ concentration (CO₂ fertilization effect) could have a positive effect on crop production (e.g., wheat) (Kimball 1986). On the other hand, projected climate change (elevated temperature, changes in precipitation pattern, drought, flood, etc.) will have a negative impact on the length of the growing season

(Emam et al. 2015; Bal et al. 2022b), crop yield (Adams et al. 1988; Ahmed et al. 2016), and stability of the agricultural sector (Agovino et al. 2019).

From a rainfed agricultural point of view, climate plays an important role in crop production (Isik, & Devadoss 2006; Harsányi et al. 2021; Aslam et al. 2017), especially in the semi-arid region (Emam et al. 2015; Clay et al. 2014). Hydroclimatic deficiencies are one of the biophysical deficiencies that negatively affected crop

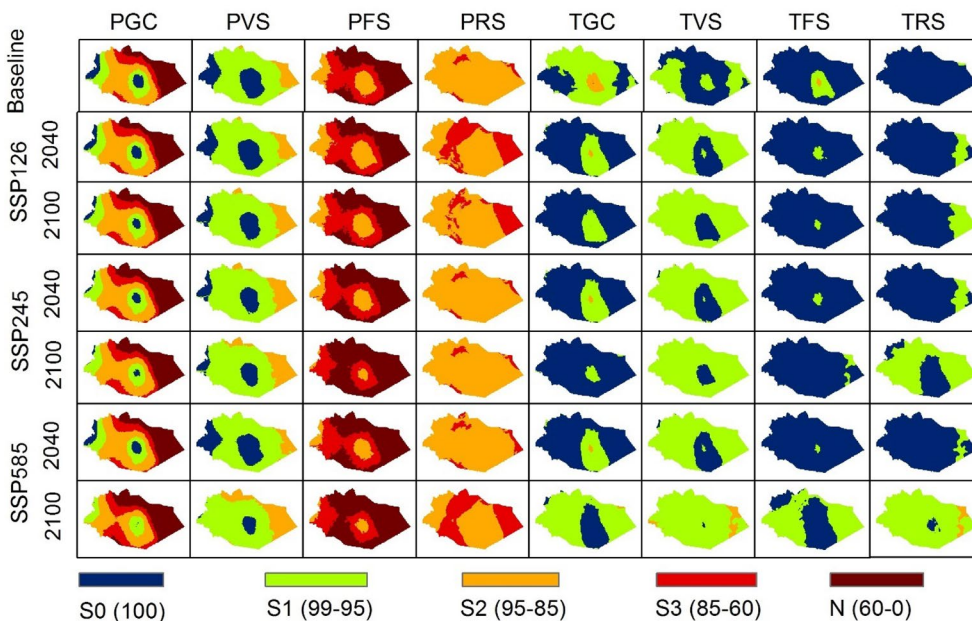


Fig. 16 Projected change of wheat agro-climatological zones during the growing cycle derived from IPSL-CM6A-LR

yield, which include unsuitable precipitation in space and time, along with high evapotranspiration (Rockström & Falkenmark 2000; Yeşilköy and Şaylan 2021). In fragile ecosystems, such as arid and semi-arid regions (like Syria), the time and amount of precipitation during the growing cycle are the important factors that determined crop yield. Precipitation during the growth cycle was regarded as the most important variable in this study, with a weightage of 0.26 to 0.4, and positively linked to wheat growth and yields. Many scholars emphasize the importance of precipitation for rainfed wheat production (van Ogtrop et al. 2014; Kumar et al. 2020; Aixia et al. 2022; Zhang et al. 2022; Lischeid et al. (2022)). It is good to mention here that the Mediterranean climate of the study area is distinguished by higher evaporation in the grain-fill period which badly affected the crop yield and grain quality (Ahmed et al. 2016; Ahmed and Hassan 2015).

Scientifically, the suitability of the current climate for any crop production could be defined through the suitability of climate factors (assuming all other factors are suitable), which include temperature and incoming radiation (Rockström & Falkenmark 2000; Jiu-jiang et al. 2022). In this sense, our results also reported that the mean temperature during the flowering stage influences the climate suitability for wheat production (Tables 2 and 3). In general, the gradual increase in air temperature has a negative impact on crop yield (Aslam et al. 2017). Hence, increased temperature due to climate change will directly increase the atmospheric water demand, which will accelerate plant transpiration, causing climate crop stress conditions (Rockström & Falkenmark 2000). However, this process is affected by many multidimensional factors, such as climate conditions, crop type (C3 or C4), and growth phase (emergence, tillering). Emam et al. (2015) reported that decreasing precipitation and increasing temperature in the semi-arid region will directly affect the groundwater recharge, and indirectly the soil water content which will inhibit crop production in the rainfed area which is supported by our findings (Table 5 and Fig. 10). Since wheat belongs to plant group C3, which can tolerate climate change to a certain extent, the projected climate change (higher temperatures) will shorten the wheat growing cycle leading to reduced biomass and yield under high emission scenarios (Aslam et al. 2017). So, the increases in temperature during the wheat growing cycle under low and medium emission scenarios in the short term (the middle of the current century) remain within the optimal limits for the growth and maturity of wheat, as can be seen in the output of all models (BCC-CSM2-MR,

CanESM5, and IPSL-CM6A-LR) under scenarios SSP126 and SSP245 for the 2020–2040 period in Fig. 8.

Our results indicated that the CMIP6 GCMs' projections under the SSP585 scenario and 2015–2100 period showed a reduction of wheat yields by -0.2 to -0.8 t/ha due to a reduction of 4–12% of WCSI greatly in the western part, i.e., by 10–30% in general. A few studies were carried out to assess the impact of climate change on wheat production in the Mediterranean Basin. For example, future climate projections based on GCMs showed a 20% decrease in wheat yield in Turkey due to low precipitation and high transpiration, as well as a shorter grain-filling period (Özdoğan 2011). In Jordan, Al-Bakri et al. (2011) projected a reduction of wheat and barley yields by 10–20% and 4–8%, due to a reduction of precipitation by 10–20%. Similarly, Nassiri et al. (2006) concluded that climate change will reduce rainfed wheat yield by 18% (in 2025) and 24% (in 2050) due to a reduction in the length of the growing cycle and a precipitation deficit. Wheat yields in Algeria tend to decrease with future climate change, with a -36% relative change in wheat yield between the future and the baseline (Chourghal et al. 2016). In contrast, Ashraf Vaghefi et al. (2014) evaluated the impact of different climate scenarios on wheat production and water resources and reported that climate change will have a positive effect in some parts and a negative in other parts; this is consistent with the findings of our study.

Conclusion

The change in a suitable area for wheat cultivation in Syria during 2020–2100 compared to 1982–2015 was estimated using a newly proposed “Weighted climate suitability index.” Weights were assigned to eight climate-related suitability criteria using the AHP and the consistency of the weights was evaluated. Future climate data derived from three GCMs from the latest CMIP6 was used for three emission scenarios, viz., SSP126, SSP245, and SSP585 for the period 2020–2100. The results indicated a decrease in area under the “extremely suitable” and “acceptable suitable” categories and an increase in area under the “moderately suitable” category for wheat production. This study has also identified that the yield reduction will be higher in western parts than in eastern and northern parts. Hence, more emphasis should be given to climate change adaptation strategies in wheat production, especially in the western parts of the study area. The results of this study will also help in the strategic planning of wheat production in Syria under the projected climate scenarios. Reports of this research are limited to small areas as a case study, although it is

not relevant to similar regions worldwide. However, the study employs novel analytical methods that can be used broadly.

Appendix

Equations appendix

In AHP method it is substantial that the weights derived from PWCM be harmonious. As such, the Weighted Sum Vector (WSV) was computed to discover the consistency or inconsistency among the studied indicators. Due to random matrix figuration, some of the inconsistencies may be present in the outputs (Saaty 1980, 1990). We used Equations (E1) and (E2) to compute the Consistency Vector (CV) by multiplying the matrix *A* by the criteria weights (Feizizadeh et al. 2014):

$$WSV = [a_{ij} * w_j], i, j = 1, 2, 3, \dots, n, \tag{E1}$$

in which the CV was derived by dividing the WSV by the criteria weights, can be expressed as

$$CV = \left[\frac{wsvj1}{wj1} \right], \left[\frac{wsvj2}{wj2} \right], \left[\frac{wsvj3}{wj3} \right], \dots \left[\frac{wsvjn}{wjn} \right]. \tag{E2}$$

The lambda value (λ_{max}) which is the maximum Eigenvalue of the matrix (Saaty 1977) being computed by the mean value of the CVs is obtained as

$$\lambda_{max} = \frac{cv1 + cv2 + cv3 + \dots cvn}{no. of criteria}. \tag{E3}$$

The consistency ratio (CR) as a coefficient of the degree of the matrix coherence and consistency was obtained, to report the likelihood of the matrix judgement and compatibility priorities were implemented randomly (Saaty 1977) is obtained as:

$$CR = \frac{CI}{RCI}. \tag{E4}$$

The RCI is the random consistency index introduced by Saaty (1980) for $n=8$, $RCI = 1.41$, and the CI is the consistency index and is being calculated as follows:

$$CI = \frac{\lambda_{max} - n}{n - 1}, \tag{E5}$$

in which the maximum Eigenvalue of the matrix (λ_{max}) was calculated by Equation (E3). The CR coefficient should be equal to 0.10 or less, indicating that the degree of cohesiveness in the PWCM is acceptable; otherwise, it is indicating that the PWCM is incompatible and should be reevaluated (i.e., when the CR coefficient is > 0.10).

Author contributions

KA contributed to conceptualization, methodology, software, formal analysis, investigation, data curation, writing—original draft preparation, and visualization. SB was responsible for supervision, project administration, funding acquisition, and writing—review and editing. HGA was involved in methodology and writing—original draft preparation. HA and MAM were involved in funding acquisition and writing—review and editing. AKS and SKB were involved in writing—review and editing. BA was involved in data curation and writing—review and editing. MASC and SM contributed to writing—original draft preparation. All the authors read and approved the final manuscript.

Funding

This work was supported by the national natural science foundation of China (under Grants 41971340 and 41271410) and by Princess Nourah bint Abdulrahman University Research Supporting Project Number PNUKSP2022R241, Princess Nourah bint Abdulrahman University, Riyadh, Saudi Arabia. The authors also acknowledge the funding by the German Federal Ministry of Education and Research (BMBF) in the framework of the funding measure “Soil as a Sustainable Resource for the Bioeconomy—BonaRes,” project BonaRes (Module A): BonaRes Center for Soil Research, subproject “Sustainable Subsoil Management—Soil3” (Grant 031B0151A), and partially funded by the Deutsche Forschungsgemeinschaft (DFG, German Research Foundation) under Germany’s Excellence Strategy—EXC 2070—390732324.

Availability of data and materials

Data are available upon request.

Declarations

Consent for publication

All the authors have read and agreed to publish this version of the manuscript.

Competing interests

The authors declare no conflict of interest.

Author details

¹School of Geographical Sciences, Nanjing University of Information Science and Technology, Nanjing 210044, China. ²Department of Geography, Faculty of Arts and Humanities, University of Tartous, Tartous, Syria. ³Department of Geography, Faculty of Arts and Humanities, Damascus University, Damascus, Syria. ⁴Department of Geography, College of Arabic Language and Social Studies, Qassim University, Burayda 51452, Saudi Arabia. ⁵Pome and Grapevine Division, Swaida, General Commission for Scientific Agricultural Research (GCSAR), Swaida, Syria. ⁶Institute of Crop Science and Resource Conservation, University of Bonn, 53111 Bonn, Germany. ⁷Department of Geography, College of Arts, Princess Nourah Bint Abdulrahman University, P.O. Box 84428, Riyadh 11671, Saudi Arabia. ⁸ICAR-Central Research Institute for Dryland Agriculture, Hyderabad 500059, India. ⁹Institution of Land Utilization, Technology and Regional Planning, University of Debrecen, Debrecen 4032, Hungary. ¹⁰Institutes for Agricultural Research and Educational Farm, University of Debrecen, Böszörményi 138, Debrecen 4032, Hungary.

Received: 23 December 2022 Accepted: 28 March 2023

Published online: 18 April 2023

References

- Abbas G, Ahmad S, Ahmad A, Nasim W, Fatima Z, Hussain S, Hoogenboom G (2017) Quantification the impacts of climate change and crop management on phenology of maize-based cropping system in Punjab, Pakistan. *Agricul Forest Meteorol* 247:42–55
- Abd-Elmabod SK, Muñoz-Rojas M, Jordán A, Anaya-Romero M, Phillips JD, Laurence J, de la Rosa D (2020) Climate change impacts on agricultural suitability and yield reduction in a Mediterranean region. *Geoderma* 374:114453
- Adams RM, Hurd BH, Lenhart S, Leary N (1998) Effects of global climate change on agriculture: an interpretative review. *Climate Res* 11(1):19–30

- Agovino M, Casaccia M, Ciommi M, Ferrara M, Marchesano K (2019) Agriculture, climate change and sustainability: the case of EU-28. *Ecol Ind* 105:525–543
- Ahmad S, Abbas G, Ahmed M, Fatima Z, Anjum MA, Rasul G, Hoogenboom G (2019) Climate warming and management impact on the change of phenology of the rice-wheat cropping system in Punjab, Pakistan. *Field Crops Res* 230:46–61
- Ahmad, A., Ashfaq, M., Rasul, G., Wajid, S. A., Khaliq, T., Rasul, F., Saeed, U., Rahman, M. H. ur, Hussain, J., Ahmad Baig, I., Naqvi, S. A. A., Bokhari, S. A. A., Ahmad, S., Naseem, W., Hoogenboom, G., & Valdivia, R. O. (2015). Impact of Climate Change on the Rice/Wheat Cropping System of Pakistan. In *Handbook of Climate Change and Agroecosystems* 3: 219–258. IMPE-RIAL COLLEGE PRESS. https://doi.org/10.1142/9781783265640_0019
- Ahmed M, Hassan F (2015) Response of spring wheat (*Triticum aestivum* L.) quality traits and yield to sowing date. *PLoS ONE* 10(4):0126097
- Ahmed M, Qadeer U, Ahmed ZI, Hassan FU (2016) Improvement of wheat (*Triticum aestivum*) drought tolerance by seed priming with silicon. *ArchivAgron Soil Sci* 62(3):299–315
- Aixia R, Weifeng Z, Anwar S, Wen L, Pengcheng D, Ruixuan H, Min S (2022) Effects of tillage and seasonal variation of rainfall on soil water content and root growth distribution of winter wheat under rainfed conditions of the Loess Plateau China. *Agricul Water Manag* 268:107533
- Al-Bakri J, Suleiman A, Abdulla F, Ayad J (2011) Potential impact of climate change on rainfed agriculture of a semi-arid basin in Jordan. *Phys Chem Earth* 36(5–6):125–134
- Alsafadi K, Mohammed S, Habib H, Kiwan S, Hennawi S, Sharaf M (2020a) An integration of bioclimatic, soil, and topographic indicators for viticulture suitability using multi-criteria evaluation: a case study in the Western slopes of Jabal Al Arab—Syria. *Geocarto Int* 35(13):1466–1488
- Alsafadi K, Mohammed SA, Ayugi B, Sharaf M, Harsányi E (2020b) Spatial-temporal evolution of drought characteristics over Hungary between 1961 and 2010. *Pure Appl Geophys* 177(8):3961–3978
- Alsafadi K, Mohammed S, Mokhtar A, Sharaf M, He H (2021) Fine-resolution precipitation mapping over Syria using local regression and spatial interpolation. *Atmos Res* 256:105524
- Alsafadi K, Bi S, Bashir B, Hagraas A, Alatrach B, Harsanyi E, Mohammed S (2022a) Land suitability evaluation for citrus cultivation (*Citrus* spp.) in the southwestern Egyptian delta: a GIS technique-based geospatial MCE-AHP framework. *Arabian J Geosci* 15(3):1–17
- Alsafadi K, Bi S, Bashir B, Mohammed S, Sammen SS, Alsalmán A, El Kenawy A (2022b) Assessment of carbon productivity trends and their resilience to drought disturbances in the middle east based on multi-decadal space-based datasets. *Remote Sens* 14(24):6237
- Alsafadi K, Bi S, Abdo HG, Al Sayah MJ, Ratonyi T, Harsanyi E, Mohammed S (2022c) Spatial-temporal dynamic impact of changes in rainfall erosivity and vegetation coverage on soil erosion in the Eastern Mediterranean. *Environ Sci Pollution Res* 13:1–19
- Al-Saleh A, Brennan CS (2012) Bread wheat quality: some physical, chemical and rheological characteristics of Syrian and english bread wheat samples. *Foods* 1(1):3–17
- Alvar-Beltrán J, Soldan R, Ly P, Seng V, Srun K, Manzanar R, Heures A (2022) Modelling climate change impacts on wet and dry season rice in Cambodia. *J Agron Crop Sci* 208(5):746–761
- Arana C, Franco IB, Joshi A, Sedhai J (2020) SDG 15 life on land In *Actioning the Global Goals for Local Impact*. Springer, Berlin
- Ashraf Vaghefi S, Mousavi SJ, Abbaspour KC, Srinivasan R, Yang H (2014) Analyses of the impact of climate change on water resources components, drought and wheat yield in semiarid regions: Karkheh River Basin in Iran. *Hydrolog Proc* 28(4):2018–2032
- Aslam MA, Ahmed M, Stöckle CO, Higgins SS, Hayat R (2017) Can growing degree days and photoperiod predict spring wheat phenology? *Front Environ Sci* 5:57
- Asseng S, Zhu Y, Basso B, Wilson T, Cammarano D (2014) Simulation Modeling: Applications in Cropping Systems. In: Van Alfen NK (ed) *Encyclopedia of Agriculture and Food Systems*. Academic Press, Cambridge
- Bal SK, Minhas PS (2017) Atmospheric Stressors: Challenges and Coping Strategies. In: Minhas P, Rane J, Pasala R (eds) *Abiotic Stress Management for Resilient Agriculture*. Springer, Berlin
- Bal SK, Sandeep VM, Vijaya Kumar P, Subba Rao AVM, Pramod VP, Srinivasa Rao Ch, Singh NP, Manikandan N, Bhaskar S (2022a) Assessing impact of dry spells on the principal rainfed crops in major dryland regions of India. *Agricul Forest Meteorol*. <https://doi.org/10.1016/j.agrformet.2021.108768>
- Bal SK, Manikandan N, Sandeep VM, Vijayakumar P, Lunagaría MM, Subba Rao AVM, Pramod VP, Singh VK (2022b) Criteria based decisions for determining agroclimatic onset of the crop growing season. *Agricul Forest Meteorol*. <https://doi.org/10.1016/j.agrformet.2022.108903>
- Barton L, Thamo T, Engelbrecht D, Biswas WK (2014) Does growing grain legumes or applying lime cost effectively lower greenhouse gas emissions from wheat production in a semi-arid climate? *J Clean Prod* 83:194–203
- Basso B, Liu L (2019) Seasonal crop yield forecast: Methods, applications, and accuracies. *Adv in Agron* 154:201–255
- Beck HE, Zimmermann NE, McVicar TR, Vergopolan N, Berg A, Wood EF (2018) Present and future köppen-geiger climate classification maps at 1-km resolution. *Sci Data*. <https://doi.org/10.1038/sdata.2018.214>
- Ben-Ari T, Adrian J, Klein T, Calanca P, Van der Velde M, Makowski D (2016) Identifying indicators for extreme wheat and maize yield losses. *Agric Meteorol* 220:130–140
- Botzen, W.J.W., van den Bergh, J.C.J.M. & Bouwer, L.M. (2010) Climate change and increased risk for the insurance sector: a global perspective and an assessment for the Netherlands *Natural Hazards* 52(3):577–598. <https://doi.org/10.1007/s11069-009-9404-1>
- Brisson N, Ruget F, Gate P, Lorgeou J, Nicoulaud B, Tayot X, Justes E (2002) STICS: a generic model for simulating crops and their water and nitrogen balances II. Model validation for wheat and maize. *Agronomie* 22(1):69–92
- Chen Y, Khan S, Paydar Z (2010) To retire or expand? a fuzzy gis-based spatial multi-criteria evaluation framework for irrigated agriculture. *J Int Comm Irrigation Drainage* 59(2):174–188. <https://doi.org/10.1002/ird.470>
- Chen Q, Liu Y, Ge Q, Pan T (2018) Impacts of historic climate variability and land use change on winter wheat climatic productivity in the North China Plain during 1980–2010. *Land Use Policy* 76:1–9
- Chipanshi A, Zhang Y, Kouadio L, Newlands N, Davidson A, Hill H, Warren R, Qian B, Daneshfar B, Bedard F, Reichert G (2015) Evaluation of the integrated canadian crop yield forecaster (ICCF) model for in-season prediction of crop yield across the canadian agricultural landscape. *Agric for Meteorol* 206:137–150
- Chourghal N, Lhomme JP, Huard F, Aidaoui A (2016) Climate change in Algeria and its impact on durum wheat. *Reg Environ Change* 16(6):1623–1634
- Clay DE, Clay SA, Reitsma KD, Dunn BH, Smart AJ, Carlson GG, Stone JJ (2014) Does the conversion of grasslands to row crop production in semi-arid areas threaten global food supplies? *Global Food Secur* 3(1):22–30
- Costinot A, Donaldson D, Smith C (2016) Evolving comparative advantage and the impact of climate change in agricultural markets: evidence from 1.7 million fields around the world. *J Polit Econ* 124(1):205–248
- Cramer W, Guiot J, Fader M, Garrabou J, Gattuso JP, Iglesias A, Xoplaki E (2018) Climate change and interconnected risks to sustainable development in the Mediterranean. *Nat Clim Change* 8(11):972–980
- Dowling P (2013) The impact of climate change on the European energy system. *Energy Policy* 60:406–417
- Emam AR, Kappas M, Hosseini SZ (2015) Assessing the impact of climate change on water resources, crop production and land degradation in a semi-arid river basin. *Hydrol Res* 46(6):854–870
- Fanzo J, Davis C, McLaren R, Choufani J (2018) The effect of climate change across food systems: Implications for nutrition outcomes. *Glob Food Sec* 18:12–19
- FAO—Food and Agriculture Organisation (1976) *A Framework for Land Evaluation*. FAO Soils Bulletin No. 32, FAO, Rome. <https://www.fao.org/3/x5310e/x5310e00.htm>
- Feizizadeh B, Blaschke T (2013) Land suitability analysis for Tabriz County, Iran: a multi-criteria evaluation approach using GIS. *J Environ Planning Manag* 56(1):1–23. <https://doi.org/10.1080/09640568.2011.646964>
- Feizizadeh B, Jankowski P, Blaschke T (2014) A GIS based spatially-explicit sensitivity and uncertainty analysis approach for multi-criteria decision analysis. *Comput Geosci* 64:81–95. <https://doi.org/10.1016/j.cageo.2013.11.009>
- Ferrise R, Toscano P, Pasqui M, Moriondo M, Primicerio J, Semenov MA, Bindi M (2015) Monthly-to-seasonal predictions of durum wheat yield over the Mediterranean Basin. *Climate Res* 65:7–21

- Fick SE, Hijmans RJ (2017) WorldClim 2: new 1-km spatial resolution climate surfaces for global land areas. *Int J Climatol* 37(12):4302–4315. <https://doi.org/10.1002/joc.5086>
- Hanif U, Syed SH, Ahmad R, Malik KA, Nasir M (2010) Economic impact of climate change on the agricultural sector of Punjab [with comments]. *Pakistan Dev Rev* 11:771–798
- Harsányi E, Bashir B, Alsilib F, Alsafadi K, Alsaman A, Széles A, Mohammed S (2021) Impact of agricultural drought on sunflower production across Hungary. *Atmosphere* 12(10):1339
- Hateffard F, Mohammed S, Alsafadi K, Enaruvbe GO, Heidari A, Abdo HG, Rodrigo-Comino J (2021) CMIP5 climate projections and RUSLE-based soil erosion assessment in the central part of Iran. *Sci Rep* 11(1):1–17
- Hijmans RJ, Cameron SE, Parra JL, Jones PG, Jarvis A (2005) Very high resolution interpolated climate surfaces for global land areas. *Int J Climatol* 25(15):1965–1978. <https://doi.org/10.1002/joc.1276>
- Huang J, Minnis P, Yan H, Yi Y, Chen B, Zhang L, Ayers JK (2010) Dust aerosol effect on semi-arid climate over Northwest China detected from A-Train satellite measurements. *Atmos Chem Phys* 10(14):6863–6872
- Huang J, Ji M, Xie Y, Wang S, He Y, Ran J (2016) Global semi-arid climate change over last 60 years. *Clim Dyn* 46(3):1131–1150
- Isik M, Devadoss S (2006) An analysis of the impact of climate change on crop yields and yield variability. *Appl Econ* 38(7):835–844
- Jiu-jiang W, Nan W, Hong-zheng S, Xiao-yi M (2022) Spatial–temporal variation of climate and its impact on winter wheat production in Guanzhong Plain China. *Computers Electronics Agric* 195:106820
- Kapsambelis D, Moncoulon D, Cordier J (2019) An innovative damage model for crop insurance, combining two hazards into a single climatic index. *Climate* 7(1):125
- Kharin VV, Flato GM, Zhang X, Gillett NP, Zwiers F, Anderson KJ (2018) Risks from climate extremes change differently from 1.5 °C to 2.0 °C depending on rarity. *Earths Future*. <https://doi.org/10.1002/2018EF000813>
- Kimball BA (1986) Influence of elevated CO₂ on crop yield. *Carbon Dioxide Enrichment of Greenhouse Crops*, vol. II. Physiology, Yield and Economics, 105–115. (Kimball, B.A., 1986a. Influence of elevated CO₂ on crop yield. In: Enoch HZ, Kimball BA (eds) *Carbon Dioxide Enrichment of Greenhouse Crops*, vol 2. CRC Press, Boca Raton, pp 105–115
- Kirithiga SM, Patel NR (2022) In-season wheat yield forecasting at high resolution using regional climate model and crop model. *AgriEngineering* 4(4):1054–1075
- Koetse MJ, Rietveld P (2009) The impact of climate change and weather on transport: An overview of empirical findings. *Transp Res Part D Transp Environ* 14(3):205–221
- Kotlowski K (2007) Qualitative models of climate variations impact on crop yields. technical Report IR-07–034. IIASA Interim Report.
- Kumar S, Roshni T, Kahya E, Ghorbani MA (2020) Climate change projections of rainfall and its impact on the cropland suitability for rice and wheat crops in the Sone river command. *Bihar Theoretical Appl Climatol* 142(1):433–451
- Le Blanc D (2015) Towards integration at last? The sustainable development goals as a network of targets. *Sustain Dev* 23(3):176–187
- Li Y, Guan K, Schnitkey GD, DeLucia E, Peng B (2019) Excessive rainfall leads to maize yield loss of a comparable magnitude to extreme drought in the United States. *Glob Change Biol* 25(7):2325–2337
- Lischeid G, Webber H, Sommer M, Nendel C, Ewert F (2022) Machine learning in crop yield modelling: a powerful tool, but no surrogate for science. *Agric for Meteorol* 312:108698
- Liu Y, Chen Q, Ge Q, Dai J, Qin Y, Dai L, Chen J (2018) Modelling the impacts of climate change and crop management on phenological trends of spring and winter wheat in China. *Agricul Forest Meteorol* 248:518–526
- Lobell DB, Asseng S (2017) Comparing estimates of climate change impacts from process-based and statistical crop models. *Environ Res Lett* 12(1):015001
- Lobell D, Cahill K, Field C (2007) Historical effects of temperature and precipitation on California crop yields. *Clim Change* 81:187–203
- Mathout S, Lopez-Bustins JA, Royé D, Martin-Vide J (2021) Mediterranean-scale drought: regional datasets for exceptional meteorological drought events during 1975–2019. *Atmosphere* 12(8):941
- Mathieu JA, Aires F (2018) Assessment of the agro-climatic indices to improve crop yield forecasting. *Agric for Meteorol* 253:15–30
- Mesta B, Sasaki H, Nakaegawa T, Kentel E (2022) Changes in precipitation climatology for the Eastern Mediterranean using CORDEX RCMs NHRCM and MRI-AGCM. *Atmospheric Res* 11:106140
- Mohammed S, Abdo HG, Szabo S, Pham QB, Holb IJ, Linh NTT, Rodrigo-Comino J (2020a) Estimating human impacts on soil erosion considering different hillslope inclinations and land uses in the coastal region of Syria. *Water* 12(10):2786
- Mohammed S, Al-Ebraheem A, Holb IJ, Alsafadi K, Dikkeh M, Pham QB, Szabo S (2020b) Soil management effects on soil water erosion and runoff in central Syria—a comparative evaluation of general linear model and random forest regression. *Water* 12(9):2529
- Mohammed S, Alsafadi K, Al-Awadhi T, Sherief Y, Harsanyie E, El Kenawy AM (2020c) Space and time variability of meteorological drought in Syria. *Acta Geophys* 68(6):1877–1898
- Mohammed S, Alsafadi K, Ali H, Mousavi SMN, Kiwan S, Hennawi S, Thai VN (2020d) Assessment of land suitability potentials for winter wheat cultivation by using a multi criteria decision support-geographic information system (MCDS-GIS) approach in Al-Yarmouk Basin (S Syria). *Geocarto Int* 12:1–19
- Mohammed S, Alsafadi K, Enaruvbe GO, Harsányi E (2022a) Assessment of soil micronutrient level for vineyard production in southern Syria. *Modeling Earth Syst Environ* 8(1):407–416
- Mohammed S, Alsafadi K, Enaruvbe GO, Bashir B, Elbeltagi A, Széles A, Harsanyie E (2022b) Assessing the impacts of agricultural drought (SPI/SPEI) on maize and wheat yields across Hungary. *Sci Rep* 12(1):8838
- Mokhtar A, Jalali M, He H, Al-Ansari N, Elbeltagi A, Alsafadi K, Rodrigo-Comino J (2021a) Estimation of SPEI meteorological drought using machine learning algorithms. *IEEE Access* 9:65503–65523
- Mokhtar A, He H, Alsafadi K, Mohammed S, Ayantobo OO, Elbeltagi A, Li Y (2021b) Assessment of the effects of spatiotemporal characteristics of drought on crop yields in southwest China. *Int J Climatol* 112:2254
- Molotoks A, Smith P, Dawson TP (2021) Impacts of land use, population, and climate change on global food security. *Food Energy Secur* 261:1145
- Mugiyo H, Chimonyo VG, Sibanda M, Kunz R, Nhamo L, Masemola CR, Mabhaudhi T (2021) Multi-criteria suitability analysis for neglected and underutilised crop species in South Africa. *PLoS ONE* 16(1):e0244734. <https://doi.org/10.1371/journal.pone.0244734>
- Mullan D (2013) Soil erosion under the impacts of future climate change: Assessing the statistical significance of future changes and the potential on-site and off-site problems. *CATENA* 109:234–246. <https://doi.org/10.1016/j.catena.2013.03.007>
- Murakami K, Shimoda S, Kominami Y, Nemoto M, Inoue S (2021) Prediction of municipality-level winter wheat yield based on meteorological data using machine learning in Hokkaido. *Japan Plos One* 16(10):e0258677
- Nassiri M, Koocheki A, Kamali GA, Shahandeh H (2006) Potential impact of climate change on rainfed wheat production in Iran: (Potentieller Einfluss des Klimawandels auf die Weizenproduktion unter Rainfed-Bedingungen im Iran). *Archives Agronomy Soil Sci* 52(1):113–124
- Navarro-Racines C, Tarapues J, Thornton P, Jarvis A, Ramirez-Villegas J (2020) High-resolution and bias-corrected CMIP5 projections for climate change impact assessments. *Sci Data* 7(1):1–14
- Nxumalo G, Bashir B, Alsafadi K, Bachir H, Harsányi E, Arshad S, Mohammed S (2022) Meteorological drought variability and its impact on wheat yields across South Africa. *Int J Environ Res Public Health* 19(24):16469
- Özdoğan M (2011) Modeling the impacts of climate change on wheat yields in Northwestern Turkey. *Agr Ecosyst Environ* 141(1–2):1–12
- Parker L, Bourgoin C, Martinez-Valle A, Läderach P (2019) Vulnerability of the agricultural sector to climate change: the development of a pan-tropical climate risk vulnerability assessment to inform sub-national decision making. *PLoS ONE* 14(3):e0213641
- Peltonen-Sainio P, Jauhainen L, Trnka M, Olesen JE, Calanca P, Eckersten H, Orlandini S (2010) Coincidence of variation in yield and climate in Europe. *Agricul Ecosyst Environ* 139(4):483–489
- Pirttioja N, Carter TR, Fronzek S, Bindi M, Hoffmann H, Palosuo T, Rötter RP (2015) Temperature and precipitation effects on wheat yield across a European transect: a crop model ensemble analysis using impact response surfaces. *Clim Res* 65:87–105
- Reidsma P et al (2009) Vulnerability and adaptation of European farmers: a multi-level analysis of yield and income responses to climate variability. *Reg Environ Change* 9(1):25–40

- Rockström J, Falkenmark M (2000) Semiarid crop production from a hydrological perspective: gap between potential and actual yields. *Crit Rev Plant Sci* 19(4):319–346
- Rosenzweig C, Parry ML (1994) Potential impact of climate change on world food supply. *Nature* 367(6459):133–138
- Saaty TL (1977) A scaling method for priorities in hierarchical structures. *J Math Psychol* 15(3):234–281. [https://doi.org/10.1016/0022-2496\(77\)90033-5](https://doi.org/10.1016/0022-2496(77)90033-5)
- Saaty TL (1990) How to make a decision: the analytic hierarchy process. *Eur J Oper Res* 48(1):9–26. [https://doi.org/10.1016/0377-2217\(90\)90057-I](https://doi.org/10.1016/0377-2217(90)90057-I)
- Saaty TL (2008) Decision making with the analytic hierarchy process. *Int J Serv Sci* 1(1):83–98. <https://doi.org/10.1504/IJSSci.2008.01759>
- Saaty TL, Vargas LG (1991) Prediction, projection and forecasting. Kluwer, Dordrecht, p 251
- Saaty TL (1980) *The Analytic Hierarchy Process*; McGrawHill: New York, NY, USA
- Saha S, Sarkar D, Mondal P, Goswami S (2021) GIS and multi-criteria decision-making assessment of sites suitability for agriculture in an anabranching site of sooin river, India. *Modeling Earth Syst Environ* 7(1):571–588. <https://doi.org/10.1007/s40808-020-00936-1>
- Seetana B, Fauzel S (2018) Investigating the impact of climate change on the tourism sector: evidence from a sample of island economies. *Tourism Rev* 112:1123
- Seker M, Gumus V (2022) Projection of temperature and precipitation in the Mediterranean region through multi-model ensemble from CMIP6. *Atmos Res* 280:106440
- Srivastava AK, Safaei N, Khaki S, Lopez G, Zeng W, Ewert F, Rahimi J (2022) Winter wheat yield prediction using convolutional neural networks from environmental and phenological data. *Sci Rep* 12(1):3215
- Swart NC, Cole JN, Kharin VV, Lazare M, Scinocca JF, Gillett NP, Winter B (2019) The canadian earth system model version 5 (CanESM5 03). *Geosci Model Dev* 12(11):4823–4873
- Sys C., Van Ranst E., Debaveye J., Beernaert F (1993) Land evaluation: crop requirements. *Agricultural Publications 7*. General Administration for Development Cooperation, Brussels.
- Tang X, Liu H (2021) Spatial-temporal distribution of climate suitability of winter wheat in North China Plain for current and future climate scenarios. *Theoret Appl Climatol* 143(3):915–930
- Tol RS (2013) The economic impact of climate change in the 20th and 21st centuries. *Clim Change* 117(4):795–808
- United Nations, (2015). *Transforming our world: The 2030 agenda for sustainable development*. New York: United Nations, Department of Economic and Social Affairs. <https://sustainabledevelopment.un.org/content/documents/21252030%20Agenda%20for%20Sustainable%20Development%20web.pdf>
- van Ogtrop F, Ahmad M, Moeller C (2014) Principal components of sea surface temperatures as predictors of seasonal rainfall in rainfed wheat growing areas of Pakistan. *Meteorol Appl* 21(2):431–443
- Voogd JH (1982) Multicriteria evaluation for urban and regional planning. *Delftsche Uitgevers Maatsch* 1:125
- Wallach D, Palosuo T, Thorburn P, Hochman Z, Andrianasolo F, Seidel SJ (2021) The chaos in calibrating crop models: Lessons learned from a multi-model calibration exercise. *Environmental Modelling Software* 145:105206
- Wang X, Huang J, Feng Q, Yin D (2020) Winter wheat yield prediction at county level and uncertainty analysis in main wheat-producing regions of China with deep learning approaches. *Remote Sensing* 12(11):1744
- Webber H, White JW, Kimball BA, Ewert F, Asseng S, Rezaei EE, Martre P (2018) Physical robustness of canopy temperature models for crop heat stress simulation across environments and production conditions. *Field Crops Res* 216:75–88
- Webber H, Lischeid G, Sommer M, Finger R, Nendel C, Gaiser T, Ewert F (2020) No perfect storm for crop yield failure in Germany. *Environ Res Lett* 15(10):104012
- Wheeler T, Von Braun J (2013) Climate change impacts on global food security. *Science* 341(6145):508–513
- Woli P, Jones JW, Ingram KT, Fraisse CW (2012) Agricultural reference index for drought (ARID). *Agron J* 104(2):287–300
- Xu Z, Han Y, Tam CY, Yang ZL, Fu C (2021) Bias-corrected CMIP6 global dataset for dynamical downscaling of the historical and future climate (1979–2100). *Scientific Data* 8(1):1–11
- Yang C, Fraga H, van Ieperen W, Santos JA (2020) Assessing the impacts of recent-past climatic constraints on potential wheat yield and adaptation options under Mediterranean climate in southern Portugal. *Agric Syst* 182:102844
- Yeşilköy S, Şaylan L (2021) Yields and water footprints of sunflower and winter wheat under different climate projections. *J Clean Prod* 298:126780
- Zhang L, Wang F, Song H, Zhang T, Wang D, Xia H, Min R (2022) Effects of projected climate change on winter wheat yield in Henan China. *J Clean Product* 379:134734

Publisher's Note

Springer Nature remains neutral with regard to jurisdictional claims in published maps and institutional affiliations.

Submit your manuscript to a SpringerOpen[®] journal and benefit from:

- Convenient online submission
- Rigorous peer review
- Open access: articles freely available online
- High visibility within the field
- Retaining the copyright to your article

Submit your next manuscript at ► [springeropen.com](https://www.springeropen.com)